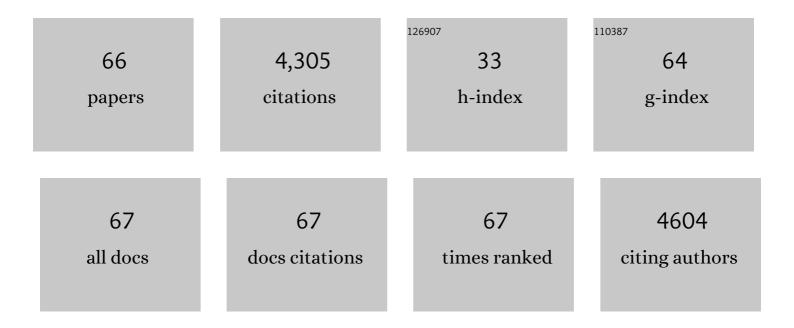
## Zhijiang Wang

List of Publications by Year in descending order

Source: https://exaly.com/author-pdf/2066902/publications.pdf Version: 2024-02-01



#	Article	IF	CITATIONS
1	Microwave absorption enhancement of porous C@CoFe2O4 nanocomposites derived from eggshell membrane. Carbon, 2019, 143, 507-516.	10.3	317
2	Electrochemical reduction of aqueous nitrogen (N <sub>2</sub> ) at a low overpotential on (110)-oriented Mo nanofilm. Journal of Materials Chemistry A, 2017, 5, 18967-18971.	10.3	241
3	SiC–Fe <sub>3</sub> O <sub>4</sub> dielectric–magnetic hybrid nanowires: controllable fabrication, characterization and electromagnetic wave absorption. Journal of Materials Chemistry A, 2014, 2, 16397-16402.	10.3	215
4	Current technology development for CO2 utilization into solar fuels and chemicals: A review. Journal of Energy Chemistry, 2020, 49, 96-123.	12.9	208
5	Ultrahigh Mass Activity for Carbon Dioxide Reduction Enabled by Gold–Iron Core–Shell Nanoparticles. Journal of the American Chemical Society, 2017, 139, 15608-15611.	13.7	191
6	Magnetite Nanocrystals on Multiwalled Carbon Nanotubes as a Synergistic Microwave Absorber. Journal of Physical Chemistry C, 2013, 117, 5446-5452.	3.1	189
7	Chemoselectivity-induced multiple interfaces in MWCNT/Fe <sub>3</sub> O <sub>4</sub> @ZnO heterotrimers for whole X-band microwave absorption. Nanoscale, 2014, 6, 12298-12302.	5.6	188
8	Eggplant-derived SiC aerogels with high-performance electromagnetic wave absorption and thermal insulation properties. Chemical Engineering Journal, 2019, 373, 598-605.	12.7	178
9	Covalent interaction enhanced electromagnetic wave absorption in SiC/Co hybrid nanowires. Journal of Materials Chemistry A, 2015, 3, 6517-6525.	10.3	163
10	Stacking fault and unoccupied densities of state dependence of electromagnetic wave absorption in SiC nanowires. Journal of Materials Chemistry C, 2015, 3, 4416-4423.	5.5	163
11	Light and Strong Hierarchical Porous SiC Foam for Efficient Electromagnetic Interference Shielding and Thermal Insulation at Elevated Temperatures. ACS Applied Materials & Interfaces, 2017, 9, 29950-29957.	8.0	163
12	Lightweight and flexible graphene/SiC-nanowires/ poly(vinylidene fluoride) composites for electromagnetic interference shielding and thermal management. Carbon, 2020, 156, 58-66.	10.3	138
13	Controllable Fabricating Dielectric–Dielectric SiC@C Core–Shell Nanowires for High-Performance Electromagnetic Wave Attenuation. ACS Applied Materials & Interfaces, 2017, 9, 40690-40696.	8.0	137
14	Black reduced porous SnO2 nanosheets for CO2 electroreduction with high formate selectivity and low overpotential. Applied Catalysis B: Environmental, 2020, 260, 118134.	20.2	107
15	Enhanced microwave absorption of Fe3O4 nanocrystals after heterogeneously growing with ZnO nanoshell. RSC Advances, 2013, 3, 3309.	3.6	106
16	Flexible, conductive, porous, fibrillar polymer–gold nanocomposites with enhanced electromagnetic interference shielding and mechanical properties. Journal of Materials Chemistry C, 2017, 5, 1095-1105.	5.5	99
17	Fabrication of core–multishell MWCNT/Fe <sub>3</sub> O <sub>4</sub> /PANI/Au hybrid nanotubes with high-performance electromagnetic absorption. Journal of Materials Chemistry A, 2015, 3, 10566-10572.	10.3	90
18	Efficient high-temperature electromagnetic wave absorption enabled by structuring binary porous SiC with multiple interfaces. Carbon, 2020, 170, 517-526.	10.3	82

ZHIJIANG WANG

#	Article	IF	CITATIONS
19	High-temperature electromagnetic wave absorption, mechanical and thermal insulation properties of in-situ grown SiC on porous SiC skeleton. Chemical Engineering Journal, 2020, 397, 125250.	12.7	77
20	Enhanced electrochemical reduction of CO <sub>2</sub> to CO on Ag electrocatalysts with increased unoccupied density of states. Journal of Materials Chemistry A, 2016, 4, 12616-12623.	10.3	74
21	Electric field-induced synthesis of dendritic nanostructured α-Fe for electromagnetic absorption application. Journal of Materials Chemistry A, 2013, 1, 4571.	10.3	63
22	Effects of fluoride on the structure and properties of microarc oxidation coating on aluminium alloy. Journal of Alloys and Compounds, 2010, 505, 188-193.	5.5	61
23	Surface Ligand Promotion of Carbon Dioxide Reduction through Stabilizing Chemisorbed Reactive Intermediates. Journal of Physical Chemistry Letters, 2018, 9, 3057-3061.	4.6	61
24	Fabrication of hydrophobic alumina aerogel monoliths by surface modification and ambient pressure drying. Applied Surface Science, 2010, 256, 5973-5977.	6.1	59
25	Blue Luminescence Emitted from Monodisperse Thiolate apped Au <sub>11</sub> Clusters. ChemPhysChem, 2009, 10, 2012-2015.	2.1	52
26	Facile Synthesis of Highly Defected Silicon Carbide Sheets for Efficient Absorption of Electromagnetic Waves. Journal of Physical Chemistry C, 2018, 122, 18537-18544.	3.1	49
27	A High-Performance Zinc-Organic Framework with Accessible Open Metal Sites Catalyzes CO <sub>2</sub> and Styrene Oxide into Styrene Carbonate under Mild Conditions. ACS Sustainable Chemistry and Engineering, 2021, 9, 2795-2803.	6.7	49
28	Preparation and Characterization of Highly Flexible Al <sub>2</sub> O <sub>3</sub> /Al/Al <sub>2</sub> O <sub>3</sub> Hybrid Composite. Journal of Nanomaterials, 2015, 2015, 1-8.	2.7	47
29	MWCNT/NiO-Fe3O4 hybrid nanotubes for efficient electromagnetic wave absorption. Journal of Alloys and Compounds, 2018, 748, 111-116.	5.5	44
30	Nature of Electromagnetic-Transparent SiO <sub>2</sub> Shell in Hybrid Nanostructure Enhancing Electromagnetic Attenuation. Journal of Physical Chemistry C, 2016, 120, 12967-12973.	3.1	40
31	Cobalt doping-induced strong electromagnetic wave absorption in SiC nanowires. Journal of Alloys and Compounds, 2019, 781, 93-100.	5.5	40
32	Dependence of reduction degree on electromagnetic absorption of graphene nanoribbon unzipped from carbon nanotube. Journal of Colloid and Interface Science, 2019, 552, 196-203.	9.4	37
33	Highly Selective Electrocatalytic Reduction of CO <sub>2</sub> into Methane on Cu–Bi Nanoalloys. Journal of Physical Chemistry Letters, 2020, 11, 7261-7266.	4.6	37
34	Large-scale gold nanoparticle superlattice and its SERS properties for the quantitative detection of toxic carbaryl. Nanoscale, 2013, 5, 5274.	5.6	33
35	Highly sensitive and selective cartap nanosensor based on luminescence resonance energy transfer between NaYF4:Yb,Ho nanocrystals and gold nanoparticles. Talanta, 2013, 114, 124-130.	5.5	32
36	A facile fabrication of a multi-functional and hierarchical Zn-based MOF as an efficient catalyst for	6.0	31

ZHIJIANG WANG

#	Article	IF	CITATIONS
37	Designed fabrication of lightweight SiC/Si3N4 aerogels for enhanced electromagnetic wave absorption and thermal insulation. Journal of Alloys and Compounds, 2022, 901, 163651.	5.5	31
38	Synergistic Chemisorbing and Electronic Effects for Efficient CO <sub>2</sub> Reduction Using Cysteamine-Functionalized Gold Nanoparticles. ACS Applied Energy Materials, 2019, 2, 192-195.	5.1	27
39	Selective CO <sub>2</sub> Electromethanation on Surface-Modified Cu Catalyst by Local Microenvironment Modulation. ACS Catalysis, 2022, 12, 8252-8258.	11.2	27
40	Durian-like multi-functional Fe3O4–Au nanoparticles: synthesis, characterization and selective detection of benzidine. Journal of Materials Chemistry A, 2013, 1, 9746.	10.3	25
41	Dicationic Ionic Liquid @MIL-101 for the Cycloaddition of CO <sub>2</sub> and Epoxides under Cocatalyst-free Conditions. Crystal Growth and Design, 2021, 21, 3689-3698.	3.0	25
42	Sizeâ€Tunable Synthesis of Monodisperse Waterâ€Soluble Gold Nanoparticles with High Xâ€ray Attenuation. Chemistry - A European Journal, 2010, 16, 1459-1463.	3.3	24
43	<i>In situ</i> fabrication of blue ceramic coatings on wrought Al Alloy 2024 by plasma electrolytic oxidation. Journal of Vacuum Science and Technology A: Vacuum, Surfaces and Films, 2012, 30, .	2.1	22
44	Effective CO2 electroreduction toward C2H4 boosted by Ce-doped Cu nanoparticles. Chemical Engineering Journal, 2022, 433, 133769.	12.7	22
45	Synergies between electronic and geometric effects of Mo-doped Au nanoparticles for effective CO <sub>2</sub> electrochemical reduction. Journal of Materials Chemistry A, 2020, 8, 12291-12295.	10.3	21
46	Ultralight, compressible, and high-temperature-resistant dual-phase SiC/Si3N4 felt for efficient electromagnetic wave attenuation. Chemical Engineering Journal, 2021, 425, 130727.	12.7	19
47	Progress and perspective of electrochemical CO2 reduction on Pd-based nanomaterials. Chemical Engineering Science, 2021, 245, 116869.	3.8	19
48	Graphene-layer-coated boron carbide nanosheets with efficient electromagnetic wave absorption. Applied Surface Science, 2021, 560, 150027.	6.1	17
49	Controllable synthesis of bifunctional NaYF4:Yb3+/Ho3+@SiO2/Au nanoparticles with upconversion luminescence and high X-ray attenuation. Journal of Alloys and Compounds, 2011, 509, 9144-9149.	5.5	16
50	Luminescent Au11 nanocluster superlattices with high thermal stability. Journal of Materials Chemistry, 2012, 22, 3632.	6.7	16
51	Ultralight, tunable monolithic SiC aerogel for electromagnetic absorption with broad absorption band. Ceramics International, 2022, 48, 26416-26424.	4.8	16
52	Growing dendritic SiC on 1D SiC nanowire: Enhancement of electromagnetic wave absorption performance. Journal of Physics and Chemistry of Solids, 2020, 136, 109124.	4.0	14
53	Theoretical insights into the factors affecting the electrochemical reduction of CO <sub>2</sub> . Sustainable Energy and Fuels, 2020, 4, 4352-4369.	4.9	14
54	Composition regulation and defects introduction via amorphous CuEu alloy shell for efficient CO2 electroreduction toward methane. Journal of CO2 Utilization, 2020, 41, 101285.	6.8	12

ZHIJIANG WANG

#	Article	IF	CITATIONS
55	In situ formation of Al2O3–SiO2–SnO2 composite ceramic coating by microarc oxidation on Al–20%Sn alloy. Applied Surface Science, 2010, 256, 3443-3447.	6.1	9
56	Exceptional size-dependent activity enhancement in the catalytic electroreduction of N2 over Mo nanoparticles. International Journal of Hydrogen Energy, 2020, 45, 31841-31848.	7.1	9
57	Direct CO2 electroreduction from NH4HCO3 electrolyte to syngas on bromine-modified Ag catalyst. Energy, 2021, 216, 119250.	8.8	9
58	Efficient CO <sub>2</sub> Electroreduction via Auâ€Complex Derived Carbon Nanotube Supported Au Nanoclusters. ChemSusChem, 2021, 14, 4929-4935.	6.8	9
59	Recent progresses in the mechanism, performance, and fabrication methods of metal-derived nanomaterials for efficient electrochemical CO <sub>2</sub> reduction. Journal of Materials Chemistry A, 2021, 9, 4558-4588.	10.3	8
60	Catalysis of solar hydrogen production by iron atoms on the surface of Fe-doped silicon carbide. Catalysis Science and Technology, 2016, 6, 7038-7041.	4.1	7
61	Self-Assembly of Amphiphilic Linearâ^'Dendritic Carbosilane Block Surfactant for Waterborne Polyurethane Coating. Polymers, 2020, 12, 1318.	4.5	7
62	Study of the Effect of PGDA Solvent on Film Formation and Curing Process of Two-Component Waterborne Polyurethane Coatings by FTIR Tracking. Coatings, 2020, 10, 461.	2.6	5
63	A Techno-Economic Study of Commercial Electrochemical CO2 Reduction into Diesel Fuel and Formic Acid. Journal of Electrochemical Science and Technology, 2022, 13, 148-158.	2.2	5
64	Effect of halogen-modification on Ag catalyst for CO2 electrochemical reduction to syngas from NH4HCO3 electrolyte. Journal of Environmental Chemical Engineering, 2021, 9, 106415.	6.7	4
65	Determination and Relaxation of Residual Stress in 2024 Al-30Âvol.% Magnesium Borate Whisker Composites. Journal of Materials Engineering and Performance, 2013, 22, 3126-3133.	2.5	3
66	Morphology characteristics and mechanical properties of hot-pressed micron/sub-micron boron carbide ceramics. Materials Today Communications, 2021, 29, 102751.	1.9	2